Effect of Hall Currents, Permeability, Heat Source and Forchhemir Parameters on Steady MHD Flow of Nano-Fluid with Rotation Through Non-Darcy Porous Medium Over Exponentially Stretching Porous Sheet

B. Tulasilakshmi Devi, B. Sreenivasa Reddy, G.V P N Srikanth

Abstract: We analyse the combined influence of Hall currents, rotation, chemical reaction and dissipation on non-Darcy convective heat and mass transfer flow of nanofluids through a porous medium past an exponentially stretching sheet .By using Runge-Kutta –Shooting method the equations have been evaluated for different variations. It is found that the linear and rotational velocities, nanoparticle volume fraction enhance with Hall pall parameter (m) and reduces with rotation parameter (R) while the temperature reduces with m and increases with R.

Key Words: Hall Currents, Rotation, Chemical Reaction, Dissipation, Non-Darcy Porous Medium, Nano-fluid.

I. INTRODUCTION

Historically, Crane (1) first considered the boundary layer flow due to linear stretching sheet. Magyari and Keller (2) studied the boundary layer flow and heat and mass transfer due to an exponentially stretching sheet. Bhattacharya and Pop (3) presented the effect of external magnetic field on the flow over an exponentially shrinking sheet. In recent years studies on Nano-fluids heat and mass transfer boundary layer laminar flow have attracted extensive attention. Choi (4) imported the nanofluids technique by using a combination of nanoparticles and the base fluids. The existence of nanoparticles in nanofluids raises thermal c onductivity and causes substantial changes in properties suc h as viscosity and specific heat compared to the base fluid.
It has involved many researchers to execute its engineering applications. Shateyi et.al (5) numerically investigated the MHD boundary layer flow with heat and mass transfer of an incompressible upper-convicted Maxwell fluid over a stretching sheet. Ibrahim et.al (6) numerically analysed the mass transfer and thermal radiation on a steady two-dimensional laminar flow of a viscous incompressible electrically conducting micropolar fluid past a stretching surface embedded in a Non-Darcian porous standard in the presence of heat generation. Nandy et.al(7) investigated the MHD boundary layer flow and heat transfer of a Non-Newtonian Caisson fluid in the neighbourhood of a stagnation point over a stretching surface in the existence of velocity and thermal slips at the edge.

Khan et.al (8) numerically calculated steady boundary layer flow past a stretching wedge with the velocity u_w (x) in a nano fluids and with a parallel free stream velocity u_e (x).Njane et.al (9) considered the magnetic field effect on boundary layer flow of a an compressed electrically conducting water-based nanofluids past a convectively heated vertical porous plate with Navier slip boundary condition. Goyal et.al (10) examined the outcome of velocity slip boundary condition on the flow and heat transfer of Non-Newtonian nanofluids over a stretching sheet with a heat source/sink, under the act of an identical magnetic field, oriented commonly to the plate. Bhattacharya et.al (1) conferred a mathematical model of the steady boundary layer flow of a nanofluids owing to an exponentially accessible stretching sheet with extraneous magnetic field. Khan et.al (12) calculated a two-dimensional steady course of an electrically conducting viscous incompressible nanofluid past a continuously moving surface in the presence of uniform transverse magnetic field with chemical reaction. Sheikhoeslam et.al (13) studied two-dimensional laminar-forced convection nanofluids flow on an enlarging surface in a permeable medium. Noghrehabad et.al (14) studied the mutual effects of Brownian motion, thermophoresis, and magnetic field on the steady boundary layer flow and heat transfer of nanofluids over a linear isothermal stretching sheet. Poornima et.al (15) examined a non-linear stretching sheet in the existence of oblique magnetic field.

Malvandi et.al (16) handled with the stable two-dimensional stagnation point flow of nano fluid towards an exponentially stretching sheet with non-uniform heat generation/absorption. Ferdows et.al (17) studied MHD boundary layer flow of nanofluids over an exponentially stretching sheet. Hamad et.al (18) analysed the boundary layer flow and heat transfer in a viscous fluid containing metallic Nano particles over a non-linear stretching sheet. Khan et.al (19) explored numerically the study of MHD radiative heat transfer in nanofluids within the authority of

Revised Manuscript Received on May 07, 2019.
B. Tulasilakshmi Devi, Professor, Department of Mathematics, CMR Institute of Technology, Hyderabad, Telangana, India.
B. Sreenivasa Reddy, Assistant Professor, Department of Applied Mathematics, Yogi Vemana University, Kadapa, A.P., India.
G.V P N Srikanth, Assistant Professor, Department of Mathematics, VNR Vignana Jyothi Institute of Engineering and Technology, Hyderabad, India

magnetic field over a stretching surface. Wahiduzzaman et.al (20) investigated numerically the viscous dissipation and radiative heat transfer in nanofluids with the influence of magnetic field over a rotating stretching surface. Takhar et.al (21) studied the flow and heat transfer on a stretching surface in a rotating fluid in the presence of a magnetic field. Sarojamma et.al (22, 23) have analysed the effect of Hall Effect, dissipation and Heat sources on convective heat and mass transfer flow of a Nano fluid past a porous stretching surface. Bhimsen kala et.al (24) analysed the combined effect of magnetic, permeability and Forchhemir parameters on steady flow of a nanofluids past a porous stretching surface.

In this paper we analyse the effect of Hall currents and rotation on the non-Darcy convective heat and mass transfer flow of a Nano fluid through a porous medium past a porous exponentially stretching surface under the influence of magnetic field .The non-linear governing equations have been solved by fourth order Runge-Kutta –Shooting technique. The velocity, rotational velocity, temperature and nanoparticle volume fraction have been discussed graphically for different variations of governing parameters. The skin friction, rate of heat and mass transfer on the wall have been evaluated numerically for different variations.

II. FORMULATION OF THE PROBLEM:

We take the steady boundary layer flow with rotational (angular) motion over a stretching sheet in an absorbent medium filled with nanofluids. A uniform magnetic field is applied normal to the plate. Assuming the magnetic Reynolds number to be small we neglect the induced magnetic field. The fluid is believed to be electrically conducting, the convicting fluid and the permeable medium are all over in thermodynamic equilibrium. It is assumed that the standardized temperature of the surface is Tw and that of the nanofluids volume fraction is Cw, the uniform temperature and nanofluids quantity fraction in the ambient(free flow region) fluid are T_∞ *and* C_∞ respectively.

The ambient (free flow region) fluid does not rotate. It is also considered that the plate is exponentially stretched with a velocity $u_w(x) = c\exp(x/L)$, where c is a positive constant and having no first rotational motion. The flow is pretended to be high so that an adjective term and a Forchheimer quadratic drag term do appear in the momentum equations. The viscous dissipation and radiation terms have not been taken into account. The physical model of the difficulty with coordinate system is as shown in the figure.1. A uniform strong magnetic field of strength B_0 is imposed along the y-axis and the effect of Hall current is taken into account. Taking Hall effects into account the generalized Ohm's law provided in the following form

$$\vec{J} = \frac{\sigma}{1+m^2}(\vec{E} + \vec{V}* + \vec{B} - \frac{1}{en_e}\vec{J} * \vec{B})$$

Where $m = \frac{\sigma B_o}{e n_c}$ is defined as the Hall current parameter. A very interesting fact that the effect of Hall current gives rise to a force in the z-direction which in turn produces a cross-flow velocity in this direction and then the flow becomes three-dimensional.

Under these assumptions, the following five field equations representing the preservation of entire mass, momentum (Brinkman-Forchheimer equations), energy and nano fluids volume part equations for the nanofluids are measured as follows:

The equation of continuity:

$$\frac{\partial u}{\partial x} + \frac{\partial v}{\partial y} = 0 \qquad (1)$$

The momentum equations:

$$u\frac{\partial u}{\partial x} + v\frac{\partial u}{\partial y} = \left(\frac{\mu}{\rho_f}\right)\frac{\partial^2 u}{\partial y^2} - \frac{\sigma\mu_e^2 B^2}{\rho_f}(u+mw) - \left(\frac{\mu}{k}\right)u - \frac{b}{\sqrt{k}}u^2 + \qquad (2)$$

$$+2\Omega w + \beta g(T-T_\infty) + \beta^* g(C-C_\infty)$$

$$u\frac{\partial w}{\partial x} + v\frac{\partial w}{\partial y} = \left(\frac{\mu}{\rho_f}\right)\frac{\partial^2 w}{\partial y^2} + \frac{\sigma\mu_e^2 B^2}{\rho_f}(mu-w) - \left(\frac{\mu}{k}\right)w - \frac{b}{\sqrt{k}}w^2 - 2\Omega u \qquad (3)$$

The equation of Energy:

$$u\frac{\partial T}{\partial x} + v\frac{\partial T}{\partial y} = k_f\frac{\partial^2 T}{\partial y^2} - \frac{Q_H}{\rho C_p}(T-T_\infty) + \frac{\nu}{C_p}\left((\frac{\partial u}{\partial y})^2 + (\frac{\partial w}{\partial y})^2\right) +$$

$$\frac{\sigma B_o^2}{\rho}(u^2+w^2) + \frac{(\rho C)_p}{(\rho C)_f} D_B\frac{\partial T}{\partial y}\frac{\partial C}{\partial y} + \frac{D_T}{T_\infty}\left(\frac{\partial T}{\partial y}\right)^2$$

(4)

The equation of Mass:

$$u\frac{\partial C}{\partial x} + v\frac{\partial C}{\partial y} = D_B\frac{\partial^2 C}{\partial y^2} + \frac{D_T}{T_\infty}\left(\frac{\partial^2 T}{\partial y^2}\right) \qquad (5)$$

Where x and y are Cartesian coordinates along the stretching wall and normal to it respectively. u and v are the velocity components along the x-axis and y-axis and w being rotational velocity about normal to x-y plane i.e about z-axis. T is the temperature in the fluid phase. C is the nanoparticle volume fraction. $B(x) = B_0\exp(x/L)$ is variable magnetic field and B_0 is constant, k is the permeability of the porous medium, b is Forchheimer coefficient, Ω is coefficient of rotational motion. ρ, ν *and* μ Are the density, kinematic viscosity and dynamic viscosity of the fluid, respectively? Further, $(\rho C_p)_f$ is the heat capacity of the fluid, $(\rho C_p)_p$ is the effective heat capacity of the nanoparticle material and k_f is the effective thermal conductivity of the porous medium. The coefficient that appears in (2.4) and (2.5) are the source coefficient Q_H, the Brownian diffusion coefficient D_B and the thermos phonetic diffusion coefficient D_T.

The boundary conditions relevant to the problem are

Published By:
Blue Eyes Intelligence Engineering
& Sciences Publication

$$y=0: u=u_w(x)=c\exp\left(\frac{x}{L}\right), v=v_w, w(x,0)=0$$
$$T=T_w=T_\infty+T_o\exp\left(\frac{x}{L}\right), C=C_w=C_\infty+C_o\exp\left(\frac{x}{L}\right)$$
$$y\to\infty: u\to 0, w(x,y)\to 0, T\to T_\infty, C\to C_\infty,$$
$$where\ u_w(x)=c\ \exp\left(\frac{x}{L}\right), v_w(x)=c\ \exp\left(\frac{x}{2L}\right) \quad (6)$$

Introducing the non-dimensional variables as

$$\eta=\left(\frac{c}{2\nu L}\right)e^{\frac{x}{2L}}y;\ \psi=(2\nu Lc)^{1/2}e^{\frac{x}{2L}}f(\eta),\ \theta(\eta)=\frac{T-T_\infty}{T_w-T_\infty};$$
$$\phi(\eta)=\frac{C-C_\infty}{C_w-C_\infty};\ u=\frac{\partial\psi}{\partial\eta};\ v=-\frac{\partial\psi}{\partial x};\ w(x,y)=ce^{\frac{x}{L}}g(\eta) \quad (7)$$

Here η is similarity variable, ψ is the stream function, θ is non-dimensional temperature, ϕ is the non-dimensional nanoparticle volume fraction.

Using (7) and Roseland approximation (*) in equation (4), the governing equations reduces to

$$f'''+ff''-2(f')^2-\frac{M^2}{1+m^2}(f'+mg_0)-D^{-1}f'+Fs(f')^2 +R1g_0+G(\theta+N\phi)=0 \quad (8)$$

$$g_0+fg_o-2f'g_0-R1f'+\frac{M^2}{1+m^2}(mf'-g_0)-D^{-1}g_0+Fs(g_0)^2=0 \quad (9)$$

$$\theta''+\Pr(f\theta'-f'\theta-Q\theta+Nb\theta'\phi'+Nt(\theta')^2+ +\Pr Ec((f'')^2+(g_o')^2)+\Pr Ec\frac{M^2}{1+m^2}(f'^2+g_o^2)=0 \quad (10)$$

$$\phi''+Le(f\phi'-f'\phi)+(\frac{Nt}{Nb})\theta''=0 \quad (11)$$

and the boundary conditions (6) *are*

$$f(0)=fw, f'(0)=1, \theta(0)=1, \phi(0)=1, g(0)=0$$
$$f'(\eta)\to 0, \theta(\eta)\to 0, \phi(\eta)\to 0, g(\eta)\to 0\ as\ \eta\to\infty \quad (12)$$

Where $fw=-v_0/\sqrt{(c\nu/2L)}$ is the wall mass transfer parameter.

fw>0 (vo<0) corresponds to mass suction and fw<0 (vo>0) corresponds to mass injection.

The parameters occurring in (8)-(11) are defined as follows

$$M=\frac{2\sigma B_o^2L}{\rho_f c}e^{-\frac{x}{L}}, D^{-1}=\frac{kce^{\frac{x}{L}}}{2L\nu}, Fs=\frac{2bL}{\sqrt{k}}, \Pr=\frac{\mu C_p}{k_f}, \nu=\frac{\mu}{\rho}$$
$$Le=\frac{\nu}{D_B}, Nb=D_B\frac{(\rho C)_p(C_w-C_\infty)}{(\rho C)_f}, Nt=\frac{D_T}{T_\infty}\frac{(\rho C)_p(T_w-T_\infty)}{(\rho C)_f},$$

$$Q=\frac{Q_H(c/2L)}{e^{-\frac{x}{L}}}, R1=\frac{4\Omega L}{U}, \gamma=\frac{k_c(c/2L)}{e^{-(\frac{x}{L})}}, U=ce^{\frac{x}{L}}$$

$Q_H=Q\ (c/2L)e^{\frac{x}{L}}$ is the non-uniform heat generation/absorption coefficient where Q>0 and Q<0 stand for heat generating and absorption parameters respectively.R1 is the fluid rotational parameter, $U=ce^{\frac{x}{L}}$ is the fluid velocity depending exponentially upon x.

The quantities of physical interest for this problem are the local skin friction due to linear motion(Cf),local skin friction due to rotation(Cg),local Nusselt number(Nux),local Sherwood number(Shx).These are defined as follows

$$C_f=\frac{\tau_w}{0.5\rho U_w^2}=\frac{\mu(\frac{\partial u}{\partial y})_{y=0}}{0.5\rho U_w^2}\Rightarrow C_f=\frac{1}{\sqrt{2R_{ex}}}f'(0)$$
$$C_g=-\frac{1}{\sqrt{2R_{ex}}}g(0), \mathrm{R}_{ex}=u_wx/\nu$$
$$Nu_x=-\frac{x(\frac{\partial T}{\partial y})_{y=0}}{T_w-T_\infty}=-\sqrt{\frac{x\mathrm{R}_{ex}}{L}}\theta'(0),$$
$$Sh_x=-\frac{x(\frac{\partial C}{\partial y})_{y=0}}{T_w-T_\infty}=-\sqrt{\frac{x\mathrm{R}_{ex}}{L}}\phi'(0)$$

III. RESULTS AND DISCUSSION

The non-dimensional linear velocity f′(η),rotational velocity g(η), temperature θ(η) and nanoparticle volume fraction ϕ(η) for various values of different parameters are exhibited in figs.2-16.

To ensure the numerical accuracy, the values of f′′(0) and f(∞) by present method are compared with the results of Magyari and Keller(18) and Krishnendu Bhattacharya and Layek (7) in Table.1 without magnetic field (M=0),non-porous media (D-1=0,Fs=0) and having no rotational motion (R=0) and with nonporous stretching sheet(s=0) and those are found to be in excellent agreement. Thus, we are very much confident that the present results are accurate.

The non-dimensional translational velocity f′(η),angular (rotational) velocity, g(η),temperature θ(η) and nanoparticle volume fraction ϕ(η) for values of Grashof number G are shown in figs.2a-2d .In the presence of mass fraction fw>0(vo<0),the translational velocity enhances and rotational velocity reduces with increase in G. This is due to the fact that the thickness of the momentum boundary layer increases with thermal buoyancy force which leads to an enhancement in f′(η)in the boundary layer. An increase in G results in a reduction of thermal boundary layer and increases the solutal boundary layer which give rise to a depreciation in temperature and an enhancement in nano particle volume fraction.

Figs.3a-3d represent the variation of f',g ,θ and ϕ with magnetic parameter M. It can be seen from the profiles that the translational velocity reduces while the rotational velocity enhances with increase in M. The increase of M leads to the increase of Lorentz force which is due to the interaction of magnetic and electric fields in the motion of an electrically conducting fluid. The weaker Lorentz force produces large resistance to the transport phenomena. The angular velocity enhances with M. Consequently, the momentum boundary layer thickness becomes thinner and the angular velocity boundary layer thickness becomes thicker. Also the temperature enhances and the nanoparticle volume fraction depreciates with M. This is due to the fact that the thickness of the thermal boundary layer increases and that of solutal boundary layer reduces for stronger magnetic field.

Figs.4a-4d exhibits the variation of f',g ,θ and ϕ withy Hall parameter(m).It is found that an increase in Hall parameter enhances the linear and rotational velocities, nanoparticle volume fraction and reduces the temperature. This is due to the fact that an increase in the Hall parameter (m) increases the thickness of the linear and rotational boundary layers and decreases the thickness of the thermal boundary layer. Also the solutal boundary layer thickness becomes thicker for higher values of Hall parameter. Fig.5a-5d show the variation of f',g ,θ and ϕ with inverse Darcy parameter D-1.The translational and angular velocities reduce with increase in D-1.Thus lesser the permeability of the porous medium smaller the velocities in the boundary layer. The temperature increase and the nanoparticle volume fraction reduces with D-1.Consequentlythe thermal boundary layer thickness becomes thicker and the nanoparticle volume faction boundary layer thickness becomes thinner for larger

Values of D-1.

Figs...6a-6d exhibit the variation of f',g ,θ and ϕ with rotation parameter (R).We find that the linear and angular velocity of the fluid decrease with increase in rotation parameter R. On the other hand, the temperature increases and the nanoparticle volume fraction reduces with increase in R. Consequently, velocity boundary thickness and angular velocity boundary layer thickness becomes thinner, and the thermal boundary layer thickness becomes thicker while the nanoparticle volume fraction boundary layer thickness becomes thinner for larger values of R. Fig.7a-7d exhibit f',g ,θ and ϕ with variation in heat source parameter Q. It can be seen from the profiles that in the presence of heat source the linear velocity, temperature decreases while the rotational velocity and nanoparticle volume fraction increases while a reversed effect is noticed in the presence of heat absorption. The is due to the fact that an increase in the fluid temperature causes more induced flow towards the plate through the thermal buoyancy effect and therefore the thickness of the thermal boundary layer is reducing for higher value of Q.

Figs.8a-8b&9a-9d exhibit f',g ,θ and ϕ with Brownian motion parameter Nb and thermos phonetic parameter Nt. We notice from the profiles that the linear and angular velocities increase with increase in Nb and Nt in the boundary layer. Consequently the thickness of the linear and angular velocity boundary layers become thicker with increase in Nb and Nt. The temperature enhances with increase in Nb and Nt, while the nanoparticle volume fraction reduces with Nb and enhances with Nt. This is due to the fact that the thickness of the thermal boundary layer increases with increase in Nb and Nt. The thickness of the nanoparticle boundary layer decreases with Nb and increases with Nt. Figs.10a-10d show the variation of f',g ,θ and ϕ with mass suction parameter fw. We find from the graphs that an increase in fw>0 enhances the linear velocity, and nanoparticle volume fraction, reduces the angular and temperature while a reversed effect is noticed in their behaviour with increase in injection parameter fw<0.

Figs.11a-11d exhibit f',g ,θ and ϕ with Forchheimer parameter Fs. It can be seen from the profiles that the linear velocity and angular velocity of the fluid increase withy increase of Forchheimer parameter Fs, except that in the region (2.0, 4.0) the angular velocity experiences a depreciation with s. The temperature reduces while the nanoparticle volume fraction enhances with increase in Fs. Consequently, the thickness of the linear and angular velocity boundary layers become thicker .The thickness of the thermal boundary layer becomes thinner while the thickness of the nanoparticle volume fraction boundary layer becomes thicker for large values of Fs. The effect of dissipation(Ec) on f',g ,θ and ϕ is noticed from figs.12a-12d.Higher the dissipation energy larger the linear, angular velocities, temperature while smaller the nanoparticle volume fraction .Consequently, the thickness of the linear and angular velocity boundary layer becomes thicker with increase in Ec. The thermal boundary layer thickness becomes thicker while that of nanoparticle volume fraction becomes thinner with higher values of Ec. Figs.13a-13d represent the variation of f',g ,θ and ϕ withy Lewis number Le. We find that an increase in Le increases the thickness of linear, angular velocities, thermal and nanoparticle volume fraction. From figs.14a-14d we find that lesser the thermal diffusivity smaller the linear, angular velocities and temperature while larger the nanoparticle volume fraction in the boundary layer.

We now discuss the variations of the physical quantities of engineering importance, that is ,the local skin friction coefficient for linear velocity, Cf, local skin friction coefficient for rotational velocity Cg and the local Nusselt number Nux, local Sherwood number for different values of G,M,D-1,m,R,Nb,Nt,Ec,,Le and pr. The quantities f′′(0),g′(0).θ′(0) and ϕ′(0) related to local skin friction coefficient for linear velocity Cf, local skin friction coefficient for rotational velocity Cg, the local Nusselt Number Nux, local Sherwood number Shx are given in table.1 for various values of parameters.

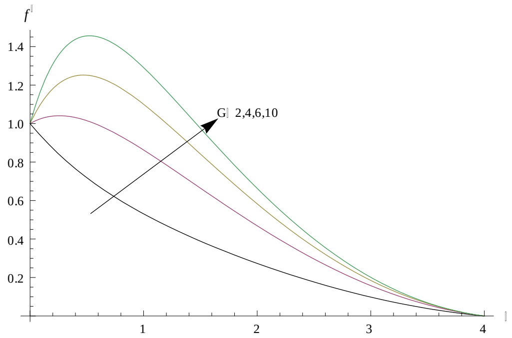

Fig.2a.Variation linear velocity(f ′) with G
M=0.5,D-1=0.2,m=0.5,Nb=Nt=0.3,Pr=0.71,Q=0.5,fw=0.2

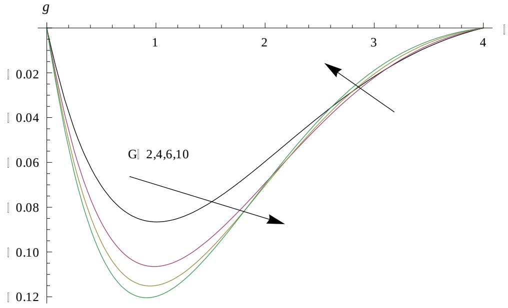

Fig.2b Variation of Rotational velocity(g) with G
M=0.5,D-1=0.2,m=0.5, Nb=Nt=0.3,Pr=0.71,Q=0.5,fw=0.2

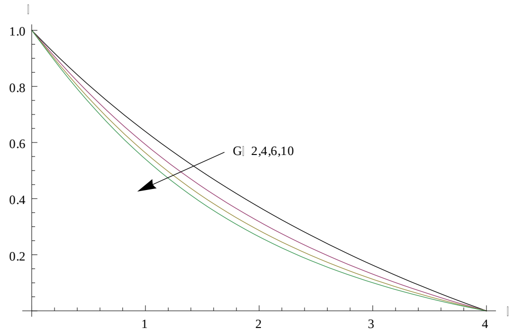

Fig.2c Variation of temperature(θ) with G
M=0.5,D-1=0.2,m=0.5,Nb=Nt=0.3,Pr=0.71,Q=0.5,fw=0.2;

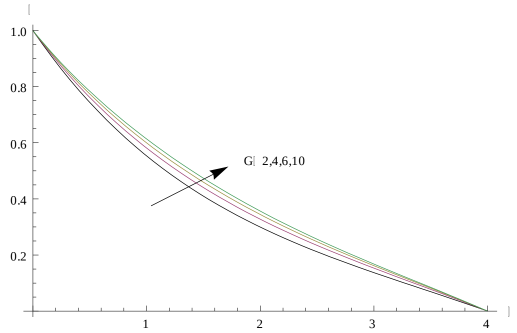

Fig.2d Variation Nanoparticle volume fraction(ϕ) with G
M=0.5,D-1=0.2,m=0.5,Nb=Nt=0.3,Pr=0.71,Q=0.5,fw=0.2;

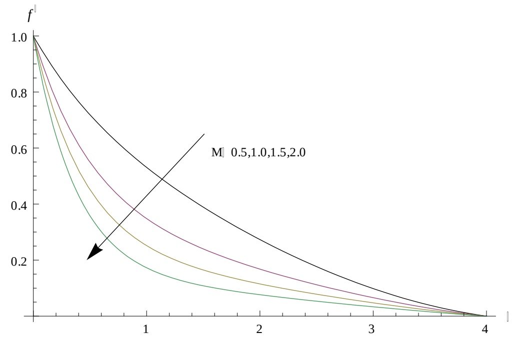

Fig.3a.Variation linear velocity(f ′) with M
G=2,D-1=0.2,m=0.5,Nb=Nt=0.3,Pr=0.71,Q=0.5,fw=0.2;

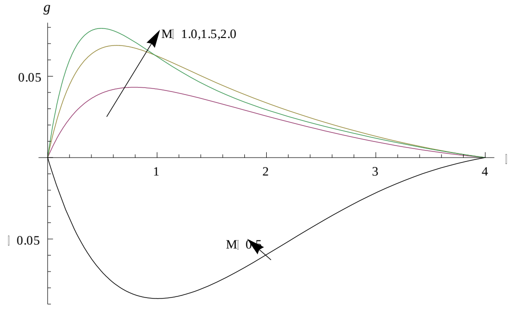

Fig.3b Variation of Rotational velocity(g) with M
G=2,D-1=0.2,m=0.5,Nb=Nt=0.3,Pr=0.71,
Q=0.5,fw=0.2, ,γ=0.5,,Fs=0.2

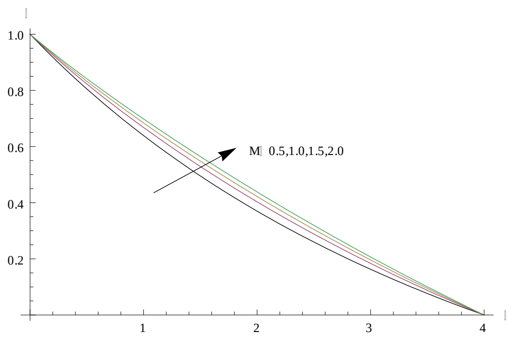

Fig.3c Variation of temperature(θ) with M
G=2,D-1=0.2,m=0.5,Nb=Nt=0.3,Pr=0.71,
Q=0.5,fw=0.2,Fs=0.2

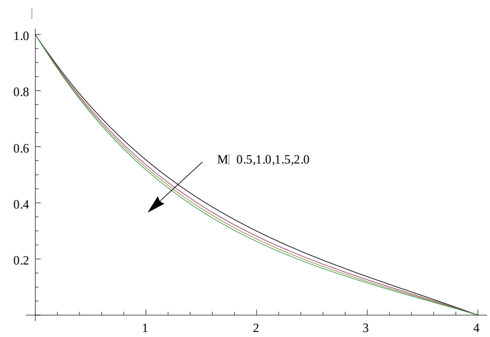

Fig.3d Variation Nanoparticle volume fraction(ϕ) with M
G=2,D-1=0.2,m=0.5,Nb=Nt=0.3,Pr=0.71,Q=0.5,fw=0.2;Fs=0.2

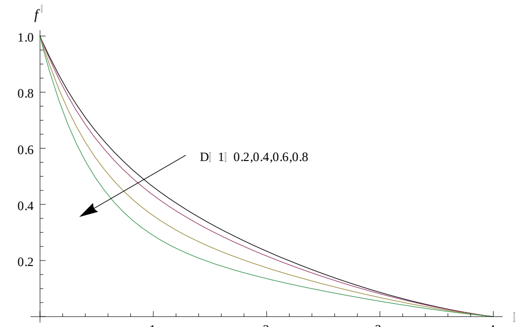

Fig.4a.Variation linear velocity(f ′) with D-1
M=0.5,D-1=0.2,m=0.5,Nb=Nt=0.3,Pr=0.71,Q=0.5,fw=0.2;Fs=0.2

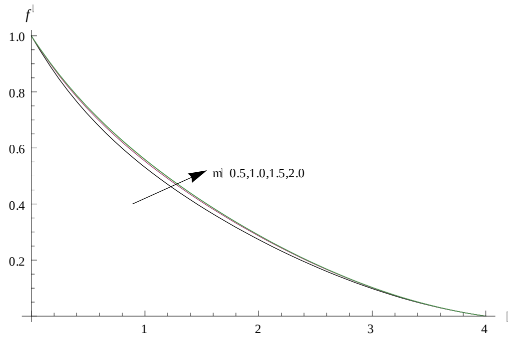

Fig.5a.Variation linear velocity(f ′) with m
M=0.5,D-1=0.2,G=2,Nb=Nt=0.3,Pr=0.71,
Q=0.5,fw=0.2; Fs=0.2

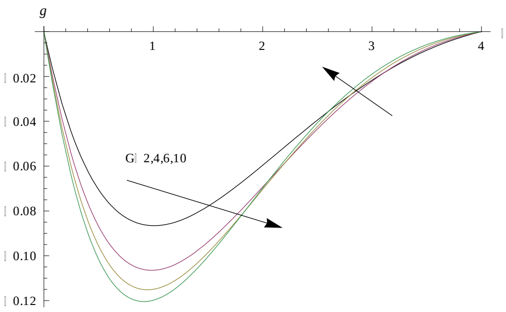

Fig.4b Variation of Rotational velocity(g) with D-1
M=0.5,G=2,m=0.5,Nb=Nt=0.3,Pr=0.71,
Q=0.5,fw=0.2, Fs=0.2

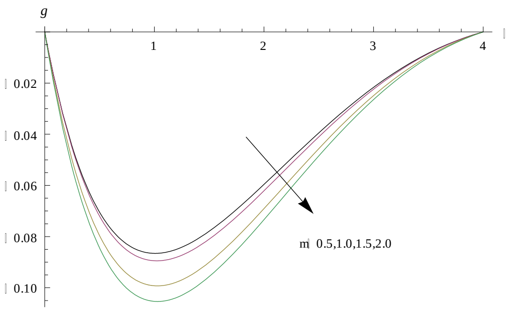

Fig.5b Variation of Rotational velocity(g) with m
M=0.5,D-1=0.2,G=2,Nb=Nt=0.3,Pr=0.71,
Q=0.5,fw=0.2,Fs=0.2

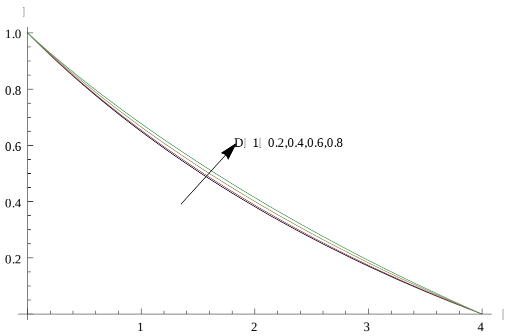

Fig.4c Variation of temperature(θ) with D-1
M=0.5,G=2,m=0.5,Nb=Nt=0.3,Pr=0.71,
Q=0.5,fw=0.2,Fs=0.2

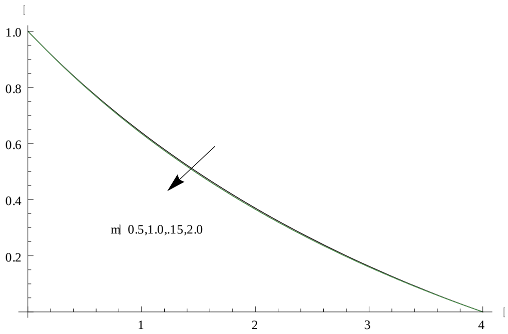

Fig.5c Variation of temperature(θ) with m
M=0.5,D-1=0.2,G=2,Nb=Nt=0.3,Pr=0.71,
Q=0.5,fw=0.2;Fs=0.2

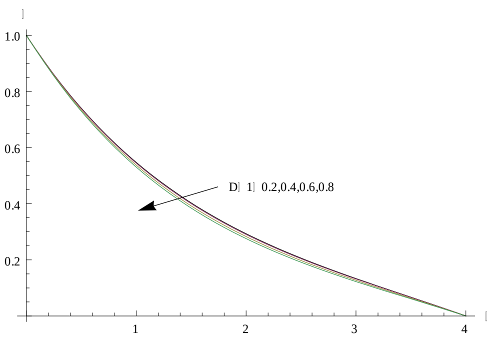

Fig.4d Variation Nanoparticle volume fraction(ϕ) with D-1
M=0.5,G=2,m=0.5,Nb=Nt=0.3,Pr=0.71,
Q=0.5,fw=0.2;Fs=0.2

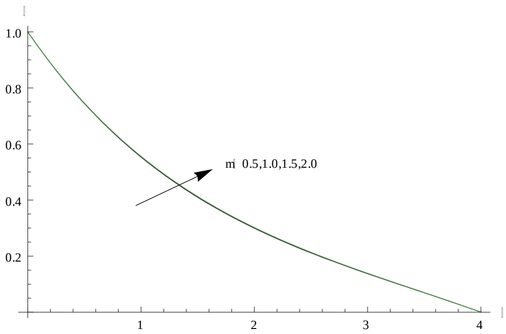

Fig.5d Variation Nanoparticle volume fraction(ϕ) with m
M=0.5,D-1=0.2,G=2,Nb=Nt=0.3,
Pr=0.71,Q=0.5,fw=0.2;Fs=0.2,Fs=0.2

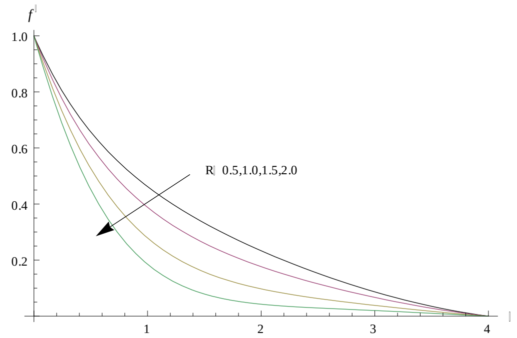

Fig.6a. Variation linear velocity(f ′) with R
M=0.5,D-1=0.2,m=0.5,Nb=Nt=0.3,Pr=0.71,
Q=0.5,fw=0.2;G=2,Fs=0.2

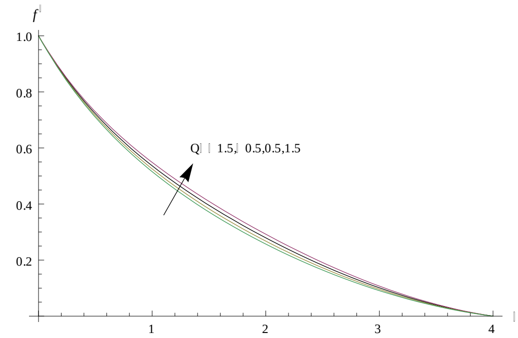

Fig7a. Variation linear velocity(f ′) with Q
M=0.5,D-1=0.2,m=0.5,Nb=Nt=0.3,
Pr=0.71,G=2,fw=0.2,Fs=0.2

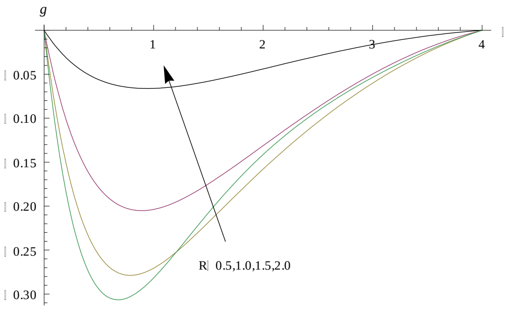

Fig.6b Variation of Rotational velocity(g) with R
M=0.5,D-1=0.2,m=0.5,Nb=Nt=0.3,Pr=0.71,
Q=0.5,fw=0.2,G=2,Fs=0.2

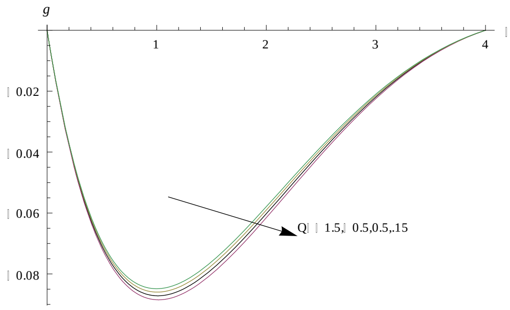

Fig.7b Variation of Rotational velocity(g) with Q
M=0.5,D-1=0.2,m=0.5,Nb=Nt=0.3,
Pr=0.71,G=2,fw=0.2,Fs=0.2

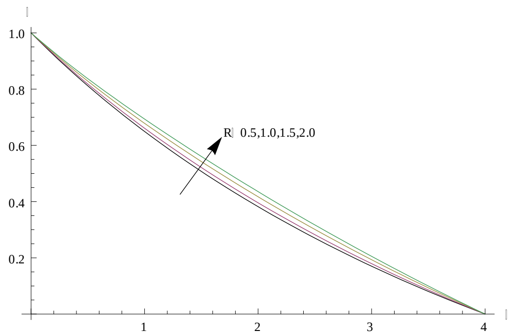

Fig.6c Variation of temperature(θ) with R
M=0.5,D-1=0.2,m=0.5,Nb=Nt=0.3,Pr=0.71,
Q=0.5,fw=0.2,G=2,Fs=0.2

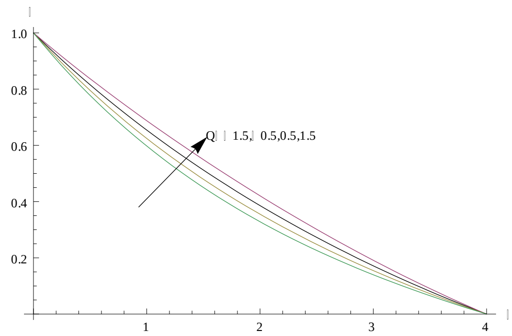

Fig.7c Variation of temperature(θ) with Q
M=0.5,D-1=0.2,m=0.5,Nb=Nt=0.3,
Pr=0.71,G=2,fw=0.2,Fs=0.2

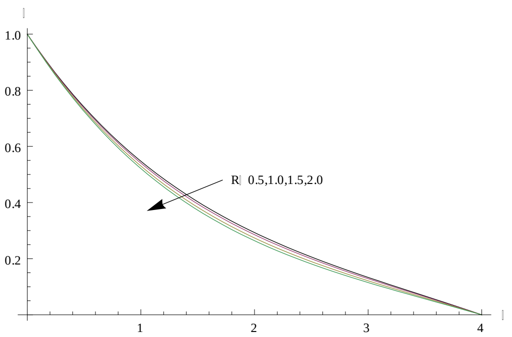

Fig.6d Variation Nanoparticle volume fraction(ϕ) with R
M=0.5,D-1=0.2,m=0.5,Nb=Nt=0.3,
Pr=0.71,Q=0.5,fw=0.2,G=2,Fs=0.2

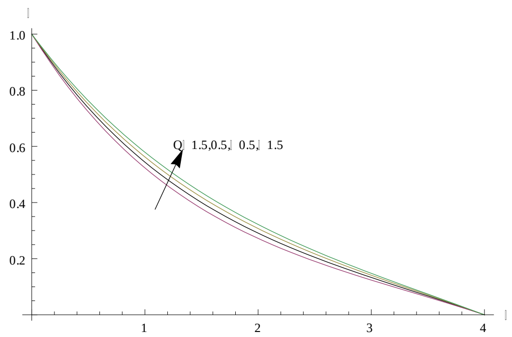

Fig.7d Variation Nanoparticle volume fraction(ϕ) with Q
M=0.5,D-1=0.2,m=0.5,Nb=Nt=0.3,Pr=0.71,
G=2,fw=0.2;Fs=0.2

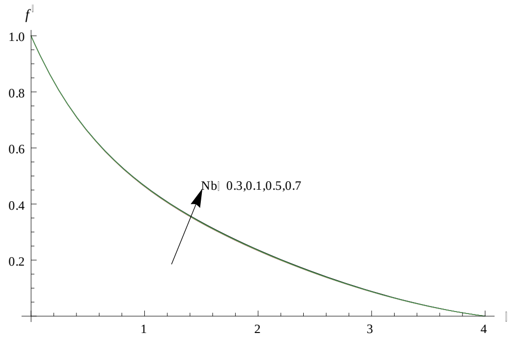

Fig.8a.Variation linear velocity(f ′) with Nb
M=0.5,D-1=0.2,m=0.5,G=2,Nt=0.3,
Pr=0.71,Q=0.5,fw=0.2;Fs=0.2

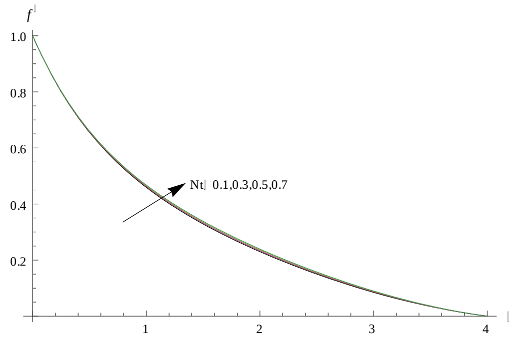

Fig.9a.Variation linear velocity(f ′) with Nt
M=0.5,D-1=0.2,m=0.5,Nb=0.3,G=2,
Pr=0.71,Q=0.5,fw=0.2;G=2,Fs=0.2

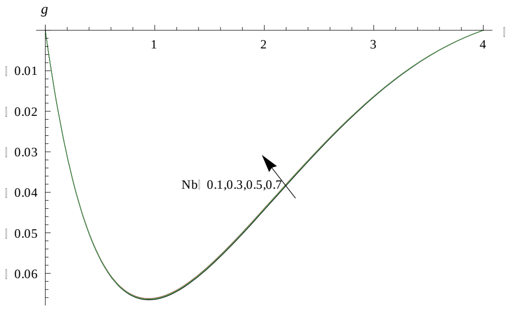

Fig.8b Variation of Rotational velocity(g) with Nb
M=0.5,D-1=0.2,m=0.5,G=2,Nt=0.3,Pr=0.71,
Q=0.5,fw=0.2,Fs=0.2

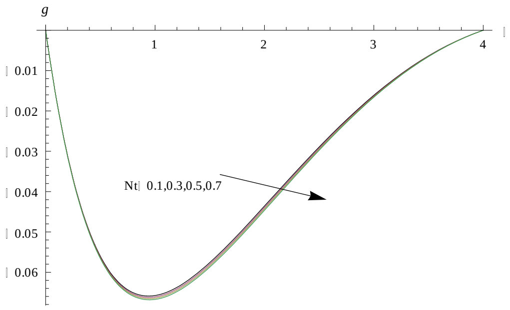

Fig.9b Variation of Rotational velocity(g) with Nt
M=0.5,D-1=0.2,m=0.5,Nb=0.3,G=2,
Pr=0.71,Q=0.5,fw=0.2,G=2,Fs=0.2

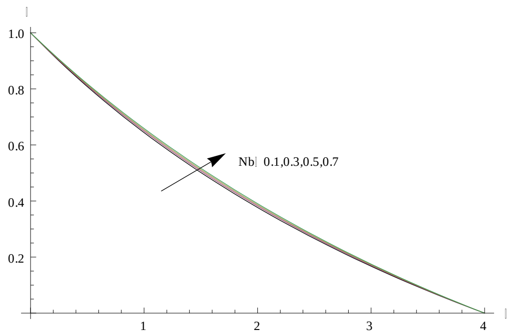

Fig8c Variation of temperature(θ) with Nb
M=0.5,D-1=0.2,m=0.5,G=2,Nt=0.3,Pr=0.71,
Q=0.5,fw=0.2;Fs=0.2

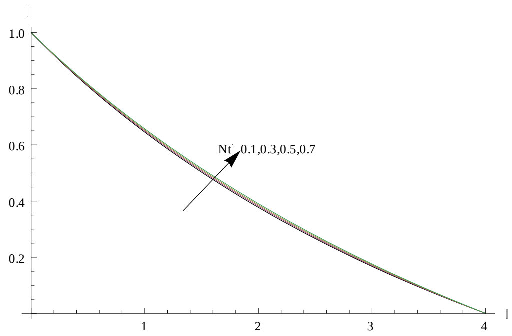

Fig.9c Variation of temperature(θ) with Nt
M=0.5,D-1=0.2,m=0.5,Nb=0.3,G=2,Pr=0.71,
Q=0.5,fw=0.2;G=2,Fs=0.2

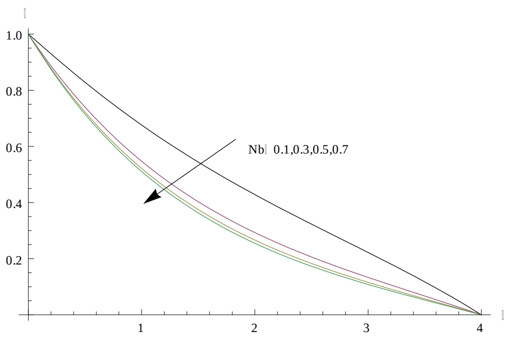

Fig.8d Variation Nanoparticle volume fraction(ϕ) with Nb
M=0.5,D-1=0.2,m=0.5,G=2,Nt=0.3,Pr=0.71,
Q=0.5,fw=0.2;fw=0.2,Fs=0.2

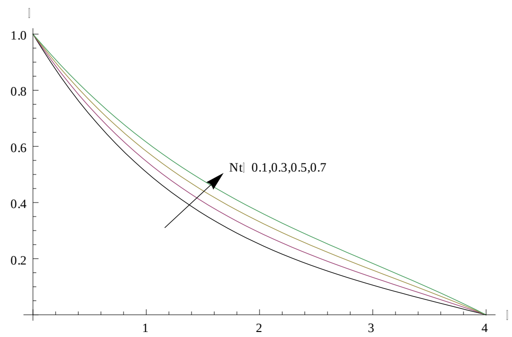

Fig.9d Variation Nanoparticle volume fraction(ϕ) with Nt
M=0.5,D-1=0.2,m=0.5,Nb=0.3,G=2,Pr=0.71,
Q=0.5,fw=0.2;G=2,Fs=0.2

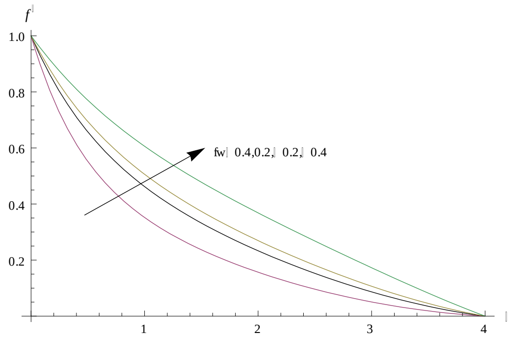

Fig.10a.Variation linear velocity(f ′) with fw
M=0.5,D-1=0.2,m=0.5,Nb=Nt=0.3,Pr=0.71,
Q=0.5,G=2;Fs=0.2,Le=2

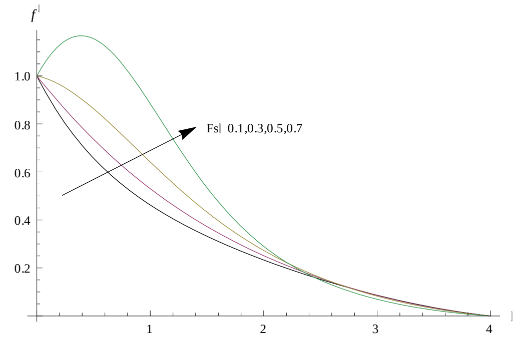

Fig.11a.Variation linear velocity(f ′) with Fs
M=0.5,D-1=0.2,m=0.5,Nb=Nt=0.3,Pr=0.71,Q=0.5,fw=0.2;G=2

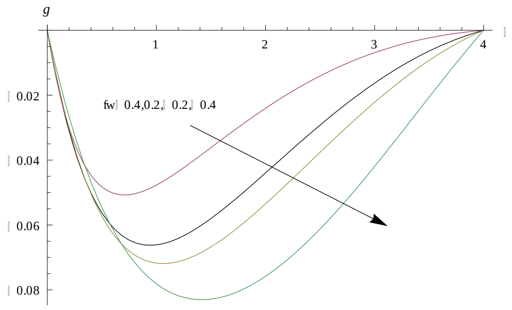

Fig.10b Variation of Rotational velocity(g) with fw
M=0.5,D-1=0.2,m=0.5,Nb=Nt=0.3,Pr=0.71,Q=0.5,G=2,Fs=0.2

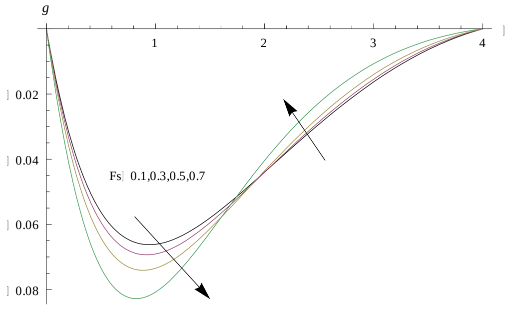

Fig.11b Variation of Rotational velocity(g) with Fs
M=0.5,D-1=0.2,m=0.5,Nb=Nt=0.3,Pr=0.71,Q=0.5,fw=0.2,G=2

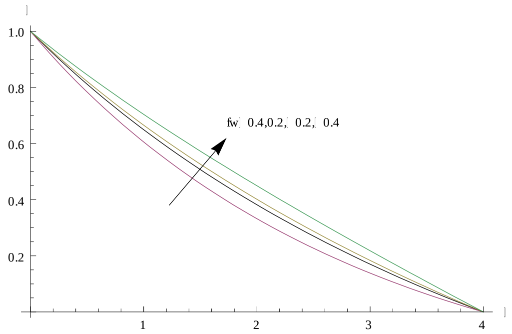

Fig.10c Variation of temperature(θ) with fw
M=0.5,D-1=0.2,m=0.5,Nb=Nt=0.3,Pr=0.71,Q=0.5,G=2;Fs=0.2

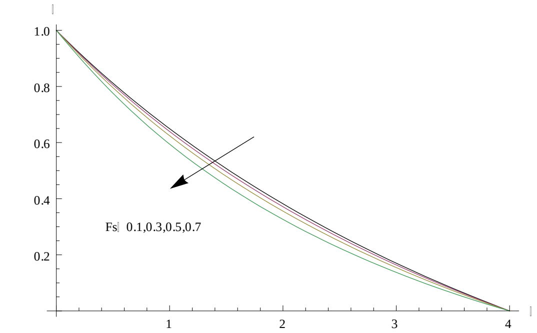

Fig.11c Variation of temperature(θ) with Fs
M=0.5,D-1=0.2,m=0.5,Nb=Nt=0.3,Pr=0.71,Q=0.5,fw=0.2;G=2

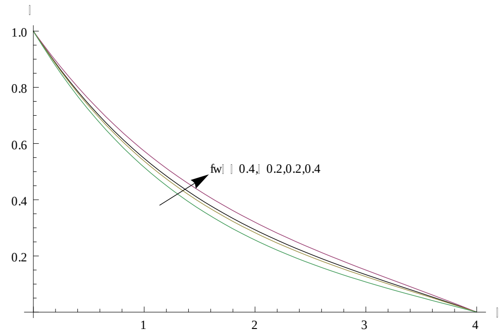

Fig.10d Variation Nanoparticle volume fraction(ϕ) with fw
M=0.5,D-1=0.2,m=0.5,Nb=Nt=0.3,Pr=0.71,Q=0.5,G=2;Fs=0.2

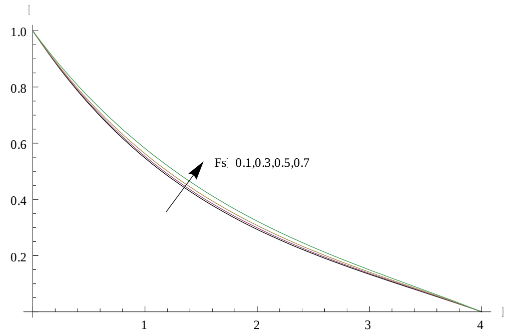

Fig.11d Variation Nanoparticle volume fraction(ϕ) with Fs
M=0.5,D-1=0.2,m=0.5,Nb=Nt=0.3,Pr=0.71,Q=0.5,fw=0.2;G=2

Published By:
Blue Eyes Intelligence Engineering
& Sciences Publication

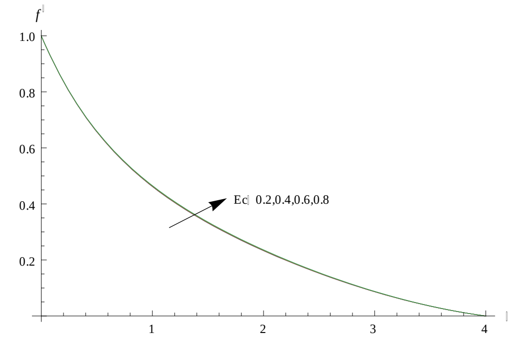

Fig.12a.Variation linear velocity(f ′) with Ec
M=0.5,D-1=0.2,m=0.5,Nb=Nt=0.3,Pr=0.71,Q=0.5,fw=0.2;Fs=0.2

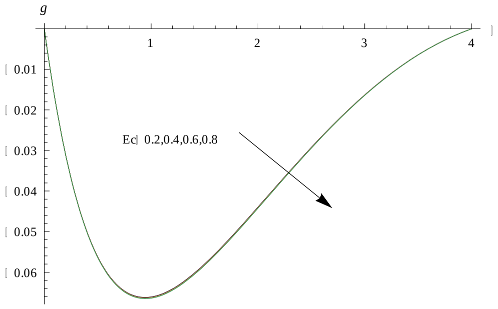

Fig.12b Variation of Rotational velocity(g) with Ec
M=0.5,D-1=0.2,m=0.5,Nb=Nt=0.3,Pr=0.71,Q=0.5,fw=0.2,Fs=0.2

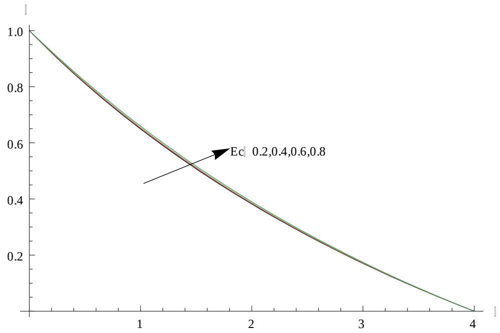

Fig.12c Variation of temperature(θ) with Ec
M=0.5,D-1=0.2,m=0.5,Nb=Nt=0.3,Pr=0.71,Q=0.5,fw=0.2;Fs=0.2

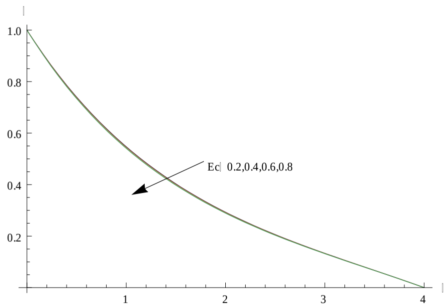

Fig.12d Variation Nanoparticle volume fraction(ϕ) with Ec
M=0.5,D-1=0.2,m=0.5,Nb=Nt=0.3,Pr=0.71,Q=0.5,fw=0.2;Fs=0.2

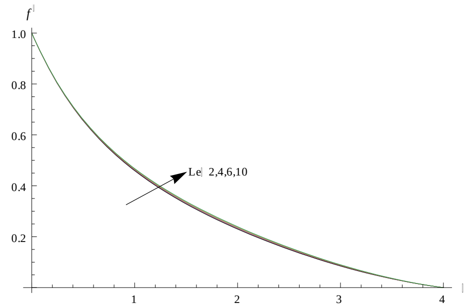

Fig.13a.Variation linear velocity(f ′) with Le
M=0.5,D-1=0.2,m=0.5, Nb=Nt=0.3,Pr=0.71,Q=0.5,fw=0.2;Fs=0.2

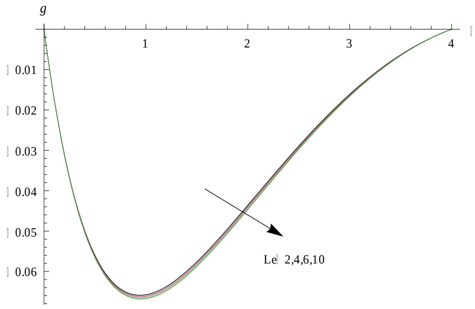

Fig.13b Variation of Rotational velocity(g) with Le
M=0.5,D-1=0.2,m=0.5,Nb=Nt=0.3,Pr=0.71,Q=0.5,fw=0.2,Fs=0.2

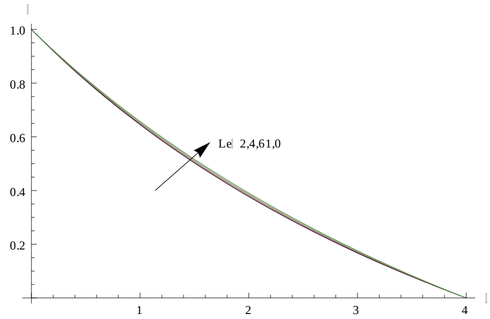

Fig13c Variation of temperature(θ) with Le
M=0.5,D-1=0.2,m=0.5,Nb=Nt=0.3,Pr=0.71,
Q=0.5,fw=0.2;Le=2,Fs=0.2

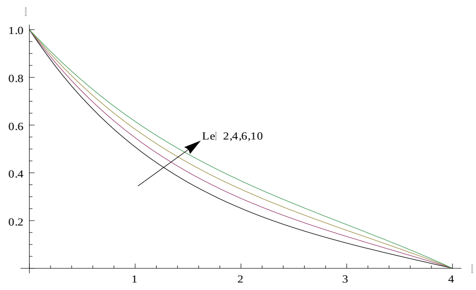

Fig.13d Variation Nanoparticle volume fraction(ϕ) with Le
M=0.5,D-1=0.2,m=0.5,Nb=Nt=0.3,Pr=0.71,
Q=0.5,fw=0.2;Le=2,Fs=0.2;

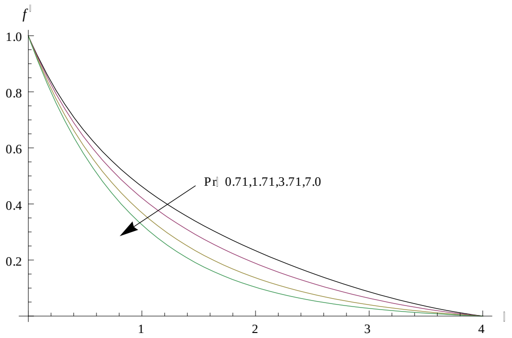

Fig.14a.Variation linear velocity(f ′) with Pr
M=0.5,D-1=0.2,m=0.5,Nb=Nt=0.3,G=2,
Q=0.5,fw=0.2;Le=2;Fs=0.2

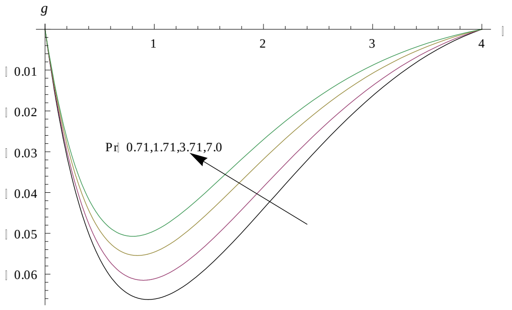

Fig.14b Variation of Rotational velocity(g) with Pr
M=0.5,D-1=0.2,m=0.5,Nb=Nt=0.3,G=2,Q=0.5,fw=0.2,fs=0.2;

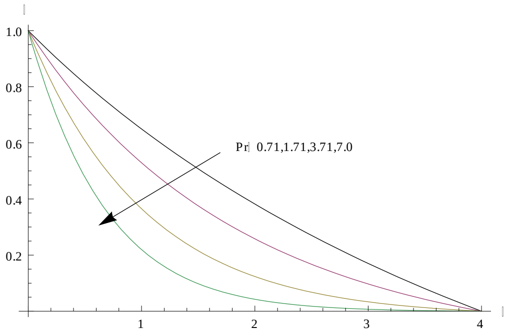

Fig.14c Variation of temperature(θ) with Pr
M=0.5,D-1=0.2,m=0.5,Nb=Nt=0.3,G=2,Q=0.5,fw=0.2;fs=0.2;

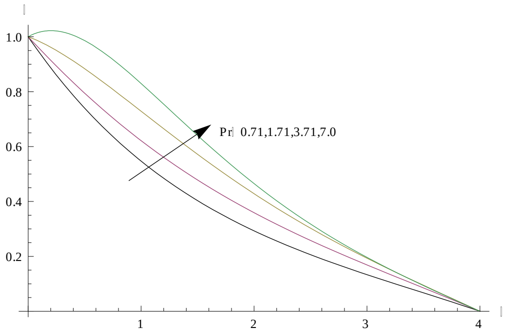

Fig.14d Variation Nanoparticle volume fraction(ϕ) with Pr
M=0.5,D-1=0.2,m=0.5,Nb=Nt=0.3,G=2,Q=0.5,fw=0.2;fs=0.2

From table.1 it is observed that the skin friction $f''(0)$,$g'(0)$ enhances with increase in G. The rate of heat and mass transfer at the wall enhance with G at the wall. An increase in magnetic parameter M enhances f'' and reduces g', in view of larger momentum exerted on the wall with higher values of M. The magnetic parameter increases the wall heat and mass transfer rate .The effect of Hall parameter on the skin friction coefficient, heat transfer and Sherwood number is exactly same as that of magnetic parameter M. The porous parameter enhances f'' and reduces g' on the wall. The rate of heat and mass transfer at the wall enhances with increase in porous parameter. When the molecular buoyancy force dominates over the thermal buoyancy force f'' reduces and g' enhances, the rate of heat and mass transfer at the wall increases when the buoyancy forces are in the same direction. Higher the rotation parameter (R) larger the f'' and g' at the wall, Nusselt number Nux and smaller Sherwood number Shx at η=0.In the presence of heat source f'' decreases and g' increases while f'' enhances and g' reduces with increase with that of strength of the heat absorption at the wall. The Nusselt number decreases and Sherwood number increases with increase in Q>0 while a reversed effect is noticed in their behaviour with increase in Q<0.The f'' reduces and g' increases at the wall for an increase in Brownian motion parameter(Nb) and thermophoretic parameter(Nt) larger f'',Nux, Shx and smaller g' at the wall. Higher the dissipation energy larger f'',Nux and g', Shx at η=0. Increasing values of Pr enhances the wall heat and mass transfer. An increase in Forchheimer parameter (Fs) reduces the skin friction coefficients and enhances the rate of heat and mass transfer at the wall.

Published By:
Blue Eyes Intelligence Engineering
& Sciences Publication

Table 1 . Skin Friction (τ_x), Nusslet number (Nu) and Sherwood Number (Sh) at η = 0

Parameter		τx(0)	τz(0)	Nu(0)	Sh(0)
G	2	-0.96665	-0.189257	0.50964	0.034058
	4	-0.31447	-0.203866	1.18538	0.302151
	6	0.156437	-0.211448	1.7338	0.486777
	10	1.33142	-0.236274	2.32272	1.03666
M	0.5	-0.96665	0.489257	0.50964	0.034058
	1.0	-1.58521	0.36689	0.75146	0.134104
	1.5	-1.95341	0.270072	0.96726	0.159948
	2.0	-2.43722	0.232709	0.988894	0.164313
m	0.5	-0.96664	-0.189257	0.50964	0.034058
	1.0	-1.02161	-0.178571	0.99854	0.152294
	1.5	-1.08183	-0.176862	1.44369	0.231682
	2.0	-1.11999	-0.151428	1.84927	0.600451
D-1	0.2	-0.96665	-0.189257	0.50964	0.034058
	0.4	-1.22771	-0.157682	0.91818	0.214044
	0.6	-1.46453	-0.134968	1.2787	0.293817
	0.8	-1.63678	-0.121699	1.62952	0.406981
Fs	0.2	-0.96665	-0.189257	0.50964	0.034058
	0.4	-0.94938	-0.179232	1.00953	0.142988
	0.6	-0.86628	-0.176017	1.49518	0.276691
	0.8	-0.58034	-0.161687	1.99046	0.728933
R	0.5	-0.96665	-0.189257	0.50964	0.534058
	1.5	-1.15948	-0.591528	0.89976	0.225478
	2.5	-1.35322	-0.893845	1.18768	0.12658
	3.0	-1.51024	-1.01597	1.72587	0.097729
Q	2	-0.70499	-0.228583	0.39709	0.610725
	4	-0.68913	-0.230426	0.34271	0.649944
	-2	-0.71933	-0.226891	0.44736	0.573979
	-4	-0.72534	-0.226175	0.46881	0.558147
Nb	0.2	-0.96641	-0.189486	0.56154	0.055437
	0.4	-1.07141	-0.17659	0.9795	0.167003
	0.6	-1.1396	-0.169212	1.34485	0.199046
	0.8	-1.58786	-0.130498	1.82105	0.185934
Nt	0.2	-0.97765	-0.18791	0.54079	0.144869
	0.4	-1.07141	-0.17659	0.9795	0.167003
	0.6	-1.12388	-0.171331	1.37043	0.750562
	0.8	-1.51918	-0.136428	1.88326	2.40967
Ec	0.1	-0.96665	-0.189257	0.50964	0.134058
	0.3	-1.06776	-0.176903	0.946	0.197261
	0.5	-1.13045	-0.170257	1.31107	0.110821
	0.7	-1.16916	-0.166871	1.61853	0.08493
Le	2	-0.96665	-0.189257	0.50964	0.134058
	4	-1.07141	-0.17659	0.9795	0.167003
	6	-1.14016	-0.169509	1.4206	0.212143
	10	-1.18452	-0.165805	1.82478	0.578604
Pr	0.71	-0.96665	-0.189257	0.50964	0.534058
	1.71	-1.07141	-0.17659	0.9795	0.167003
	3.71	-1.14016	-0.169509	1.4206	-0.212143
	7.0	-1.18452	-0.165805	1.82478	-0.578604

IV. CONCLUSIONS

We analyse the effect of heat sources and dissipation on convective heat and mass transfer flow past an exponentially stretching sheet. The nonlinear governing equation has been solved by Runge-Kutta fourth order shooting technique. From the graphical and tabular representation we find that

- An increase in Hall parameter enhances the linear and rotational velocities, nanoparticle volume fraction and reduces the temperature.

- The linear and angular velocity of the fluid decrease with increase in rotation parameter R. On the other hand, the temperature increases and the nanoparticle volume fraction reduces with increase in R.
- In the presence of heat source the linear velocity, temperature decreases while the rotational velocity and nanoparticle volume fraction increases while a reversed effect is noticed in the presence of heat absorption
- Higher the dissipation energy larger the linear, angular velocities, temperature while smaller the nanoparticle volume fraction.

REFERENCES

1. Crane,L.J:Flow past a stretching plate., Zeitschrift fur Angewandte Mathematik und Physik ZAMP,V.21,No.4,pp.645-647(1970)
2. Magyari,E and Keller,B::Heat and mass transfer in the boundary layers on an exponentially stretching continuous surface.,Journal of Physics D,V.32,No.5,pp.577-585(1999)
3. Bhattacharya K and Pop,I:MHD boundary layer flow due to an exponentially shrinking sheet,Magnetohydrodynamics,V.47,pp.337-344(2011)
4. Choi,S.U.S:Enhancing thermal conductivity of fluids with nanoparticles,Proceedings of the ASME International Mechanical Engineering Congress and Exposition,V.66,pp.99-105,San Francisco Calif,USA,November(1995)
5. Shateyi,S and Marewo,G.T:A new Numerical Approach of MH flow with Heat and Mass transfer for the UCM Fluid over a stretching surface in the presence of thermal radiation.,Hindwai Publishing Corporation, Mathematical Problems in Engineering ,V.2013,Article ID 670205,8 pages(2013)
6. Ibrahim,S.M:,Reddy,T.S and Reddy,N.B: Radiation and mass transfer effects on MHD free convection flow of a micropolar fluid past a stretching surface embedded in a Non-Darcian porous medium with heat generation.,ISRN Thermodynamics,V.2013,Article ID 534750,15 pages(2013)
7. Nandy,S.K:Analytical solution of MHD stagnation point flow and heat transfer of Casson fluid over a stretching sheet with partial slip,Hindawi Publishing Corporation ISRN Thermodynamics,V.2013,Article ID 108264,9pages(2013)
8. Khan,W.A and Pop,I:Buoyancy layer flow past a Wedge moving in a Nanofluid., Hindawi Publishing Corporatiuon Mathematical Problems in Engineering,V.2013,Article ID 637285,7 pages (2013)
9. Njane,W.N and Daniel,O: Combined effect of buoyancy force and Navier slip on MHD flow of a Nanofluid over a convectively heated vertical porous plate,Hindawi Publishing Corporation,The Scientific World Journal ,V.2013,Areticle ID 725643,8 page(2013)
10. Goyal ,M and Rama Bhargava: Numerical solution of MHD viscoelastic Nanofluid flow over a stretching sheet with partial slip and heat source/sink.,Hindawai Publishing Corporation,ISRN Nanotechnology,V.2013,Article ID 10211,11 pages(2013)
11. Bhattacharya,K and Layek,G.C: Mgnetohydrodynamic boundary layer flow of nanofluids over an exponentially stretching permeable sheet.,Hindawi Publishing Corporation,Physis Research International,V.2014,Article ID 592536,12pages(2014)
12. Khan,Md.S,Karim,I and Islam,Md.S: Possessions of chemical reaction on MHD heat and mass transfer Nanofluid flow on a continuously moving surface,American Chemical Science Journal,V.4(3),pp.401-415(2014).
13. Sheikholeslam,M and Ganji,D.D :Heated permeable stretching surface in a porous medium using Nanofluids.,Journal of Applied Fluid Mechanics,V.7,No.3,pp.535-542(2014)
14. Noghrehabadi,A,Ghalambaz,M and Ghanbarzadeh,A:Heat transfer of magnetohydrodynamic viscous nanofluids over an isothermal stretching sheet.,Journal of Thermopysics and Heat transfer,V.26,No.4(2012)
15. Poornima,T and Reddy,N.B:Radiation effects on MHD free convective boundary layer flow of nanofluids over a nonlinear stretching sheet,Advances in Applied Science Research,V.4(2),pp.190-202(2013)
16. Malvandi,A,Headyati,F,and Domairry,G:Stagnation point flow of a Nanofluid towards an exponentially stretching sheet with Non-Uniform heat generation/absorption.,Hindawi Publishing Corporation ,Journal of thermodynamics,V.2013,Article ID 764827,12 pages(2013)
17. Ferdows,M,Khan,Md,S Alam,Md.M and Sun,S:MHD mixed convective boundary layer flow of a nanofluids through a porous medium due to an exponentially stretching sheet ,Hindawi Publishing Corporation,Mathematical problems in Engineering,V.2012,Article ID 408528,21 pages,doi:10.1155/2012/408528(2012)
18. Hamad ,M Ferdows,A.A.M:Similarity solutions to viscous flow and heat transfer of nanofluids over nonlinearly stretching sheet.,Appl.Math.Mech.Eng.Ed,V.33(7),pp.923-930DOI.10.1007/s10483-012-1595-7(2012).
19. Khan,Md Shakhnoath,Md,Alam,M and Ferdows,M:MHD radiative boundary layer flow of a nanofluids past a stretching sheet.,Proceedings of the International Conference on Mechanical Engineering and Renewable Energy 2011,(ICMERE2011),22-24 December2011,Chttagong,Bangkadesh
20. Wahiduzzaman,M Shakhaoath,Md Khan,Biswas,P ,Ifsana Karim,Udd,M.S: Viscous Dissipation and radiation effects on MHD boundary layer flow of a Nanofluid past a rotating stretching sheet, Applied Mathematics,(2015),V.6,pp.547-567, http://dx.doi.org/10.423/aqm2015.63050(2015)
21. Takhar,H.S Chamkha,A.J and Nath,G:Flow and heat transfer on a stretching surface in a rotating fluid with a magnetic field, International Journal of Thermal Science,V.42,pp.23-31(2003)
22. Sarojamma,G,Syed Mahaboobjan and Nagendramma,V:Influence of Hall currents on cross diffusive convection in a MHD boundary layer flow on stretching sheet in porous medium with heat generation., International Journal of Mathematical Archieve,V.6(3),pp.227-248(2015)
23. Sarojamma,G,Syed Mahaboobjan and Sreelakshmi,K:Effect of Hall current on the flow induced by a stretching surface., International journal of Scientific and Innovative Mathematical Research,V.3(3),pp.1139-1148(2015)
24. Bhim Sen Kala, Rawat M.S. and Komal: Effect of magnetic, permeability and forchhemir parameters on steady MHD flow of nanofluids with rotation through non-darcy porous medium over exponentially stretching porous sheet, Int.J. Of Math.Archive, 6(9), p.133-146, (2015).

Published By:
Blue Eyes Intelligence Engineering
& Sciences Publication